Supporting Information:

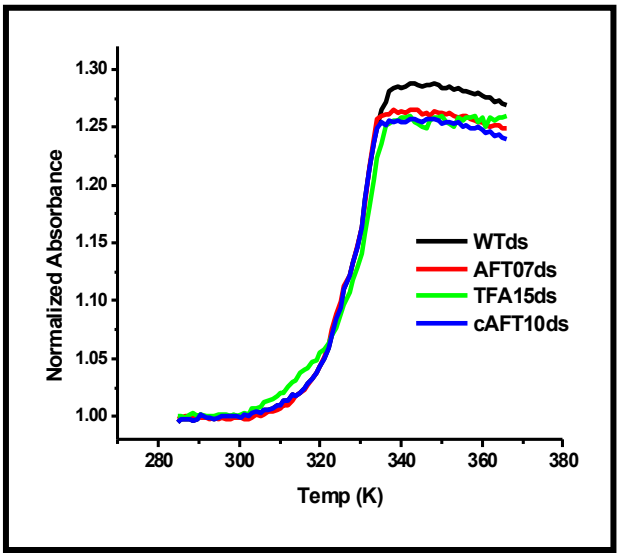

Figure S1. Thermal stability of duplexes containing 6-MI. The temperature-dependent melting curve monitored at 260 nm of the WT 34bp dsDNA (black) based on the H1 consensus binding sequence of Integration Host Factor (IHF). Also shown are curves generated with dsDNA containing 6MI, AFT07ds (red), TFA15ds (green), and cAFT10ds (blue). A similar Tm (330±1.0K) is obtained for all the duplexes, demonstrating that introduction of 6-MI does not perturb DNA stability.

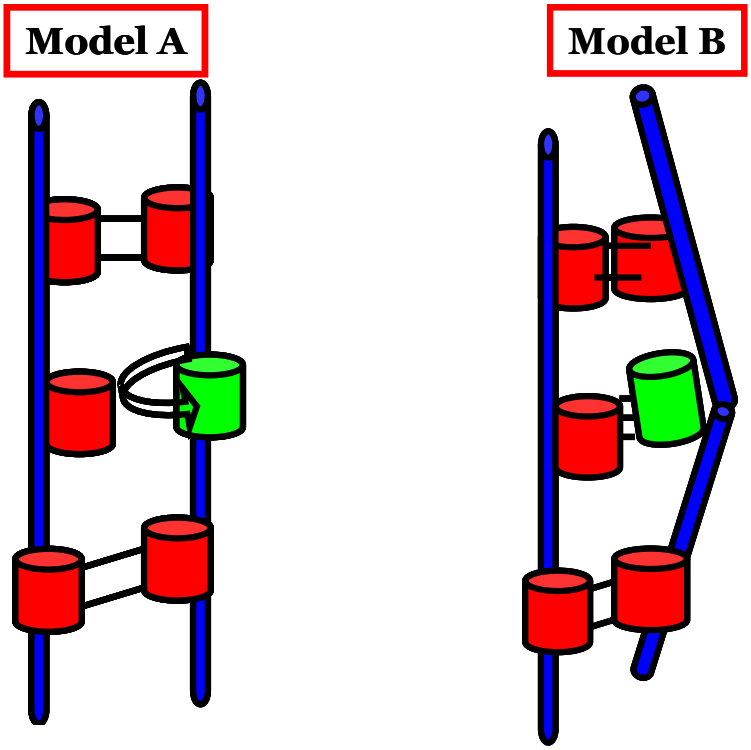

Figure S2. The proposed models for enhancement of 6-MI fluorescence. Model A: 6-MI is largely extrahelical, an environment similar to the monomer. Model B: 6-MI is in a sterically constrained conformation with minimal interaction with adjacent bases.

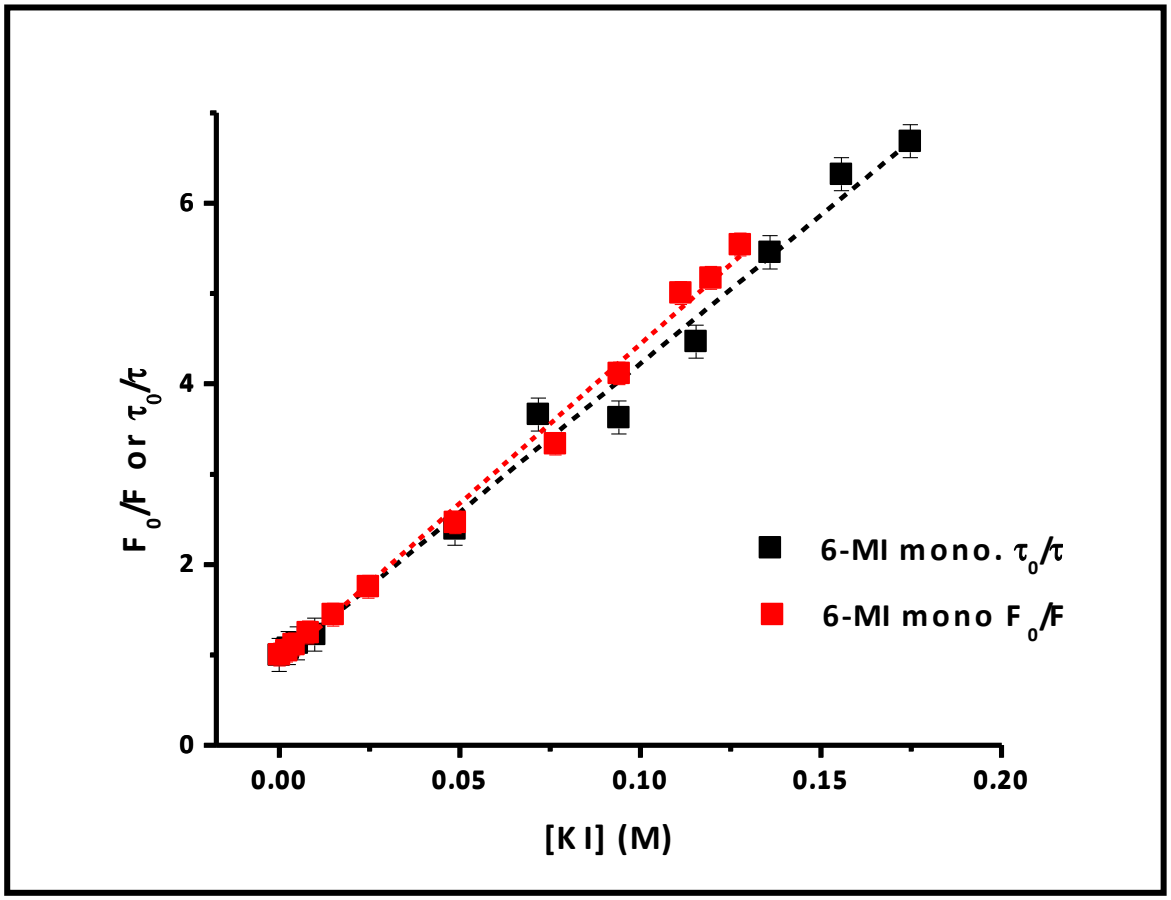

Figure S3 KI quenching of 6-MI monomer. Comparison between the excited state (τ_0/τ) and steady-state (F_0/F) KI quenching of 6-MI monomer fluorescence demonstrates there is minimal difference in the extent of quenching. The similarities in quenching rates suggest KI quenching is largely collisional.

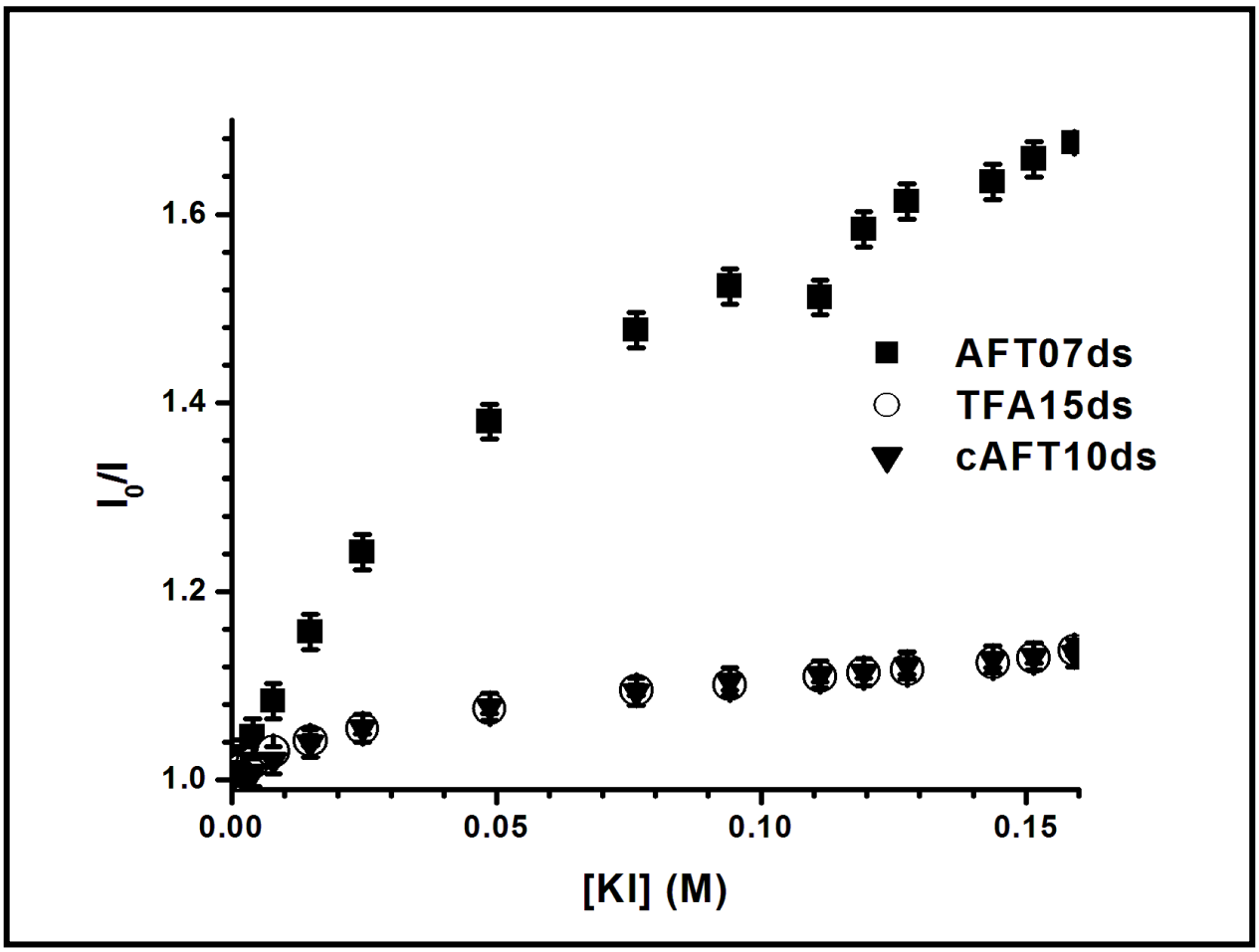

Figure S4. The Stern-Volmer plots of KI quenching of duplex DNA (AFT07ds, TFA15ds, and TFA07ds) demonstrate non-linear quenching of 6-MI when incorporated into duplex DNA. Deviation from linearity suggests a fraction of the population is not accessible to quencher

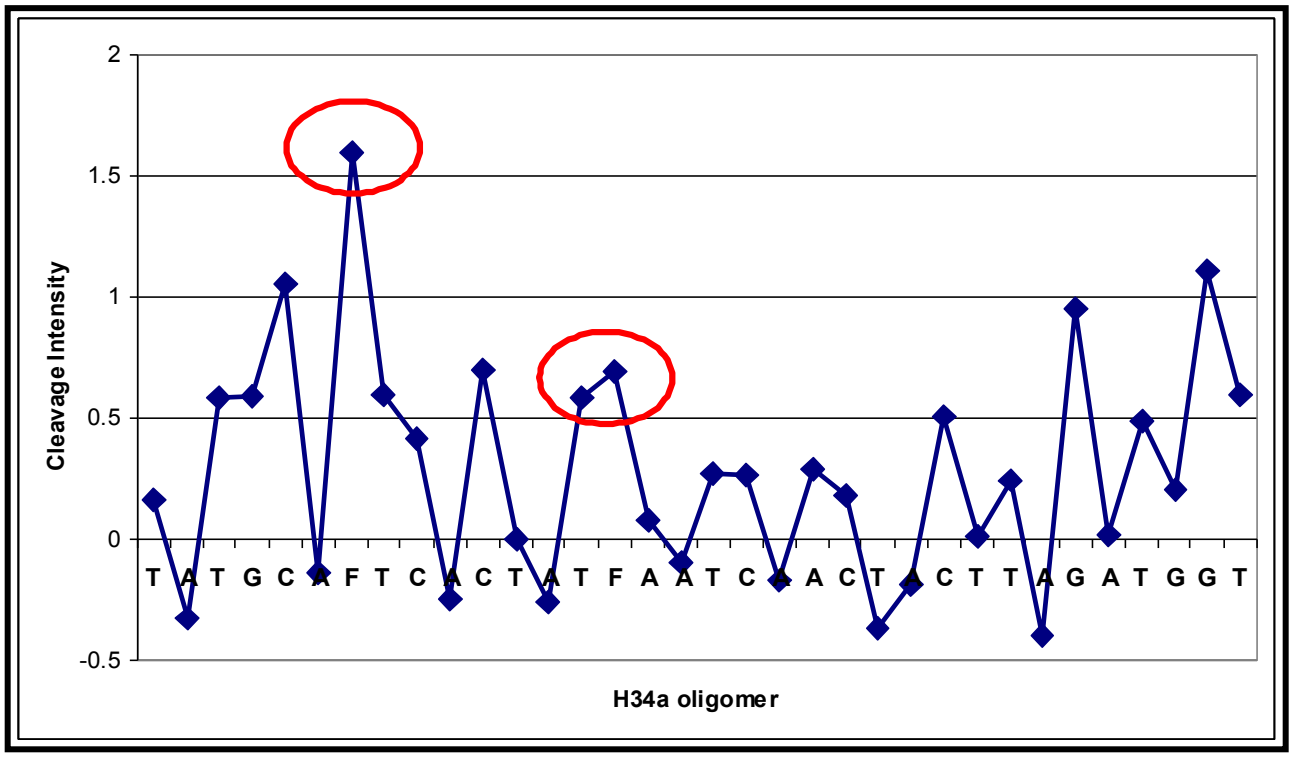

Figure S5. Cleavage intensity for WT oligomer determined using (O)H (R)adical (C)leavage (I)ntensity (D)atabase (ORChID database). There is a correlation between the larger degree of cleavage observed for the AFT07 position (1.6) compared to the TFA15 position (0.69) and the solvent accessibility determined from KI quenching experiments.

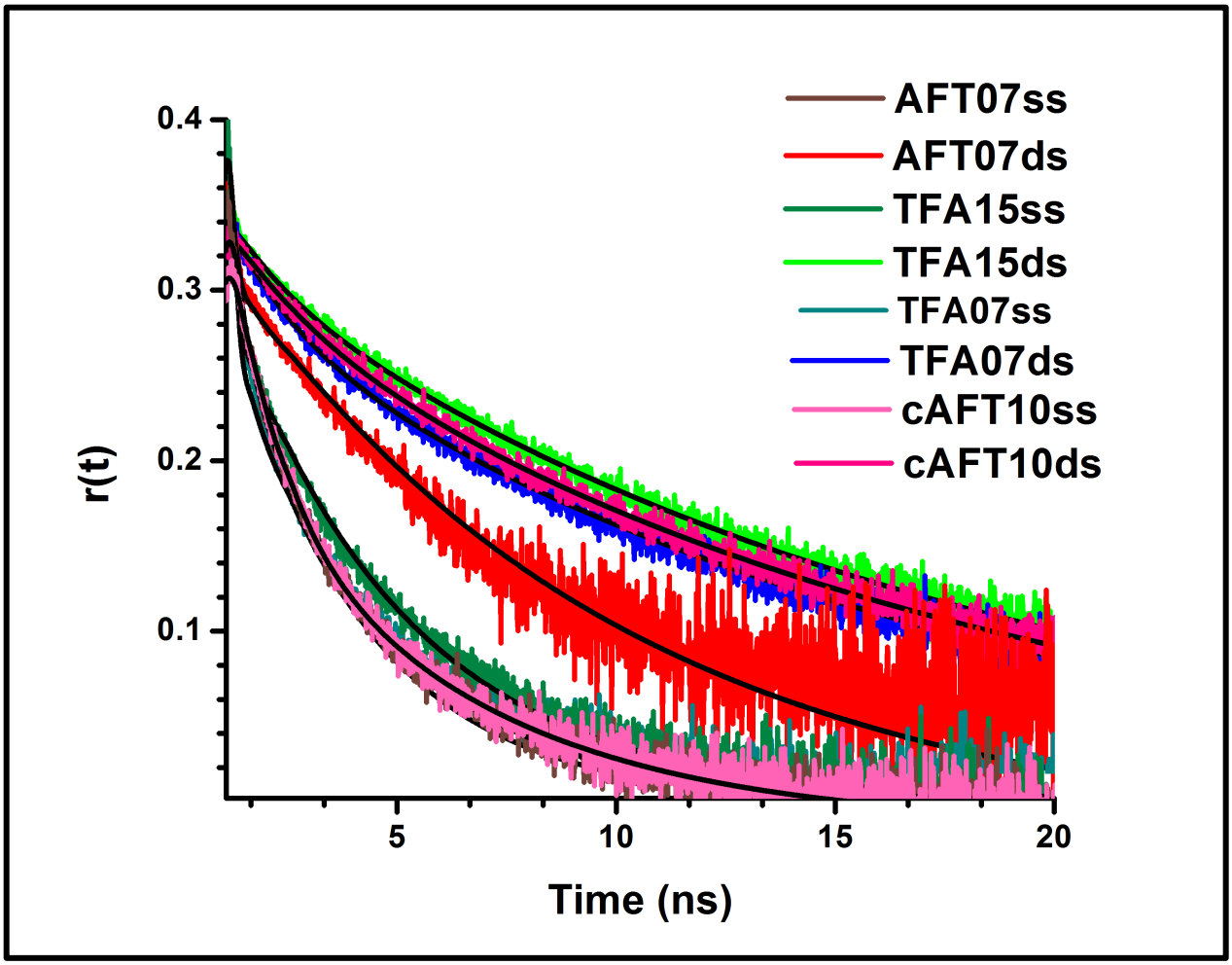

Figure S6. 6-MI local motion in ssDNA and dsDNA. Time-dependent anisotropy decay curves of 6-MI (ex=375nm, em=460nm) demonstrate the limited local motion of the 6-MI in the dsDNA sequences containing the pentamer sequences (green, blue, magenta). The time-dependent anisotropy of ssDNA (brown, dark green, teal and pink) is a bi-exponential decay composed of the local motion of 6-MI (~200ps) and the overall tumbling of DNA. Duplex formation (red, green, blue, magenta) leads to slower tumbling of DNA.

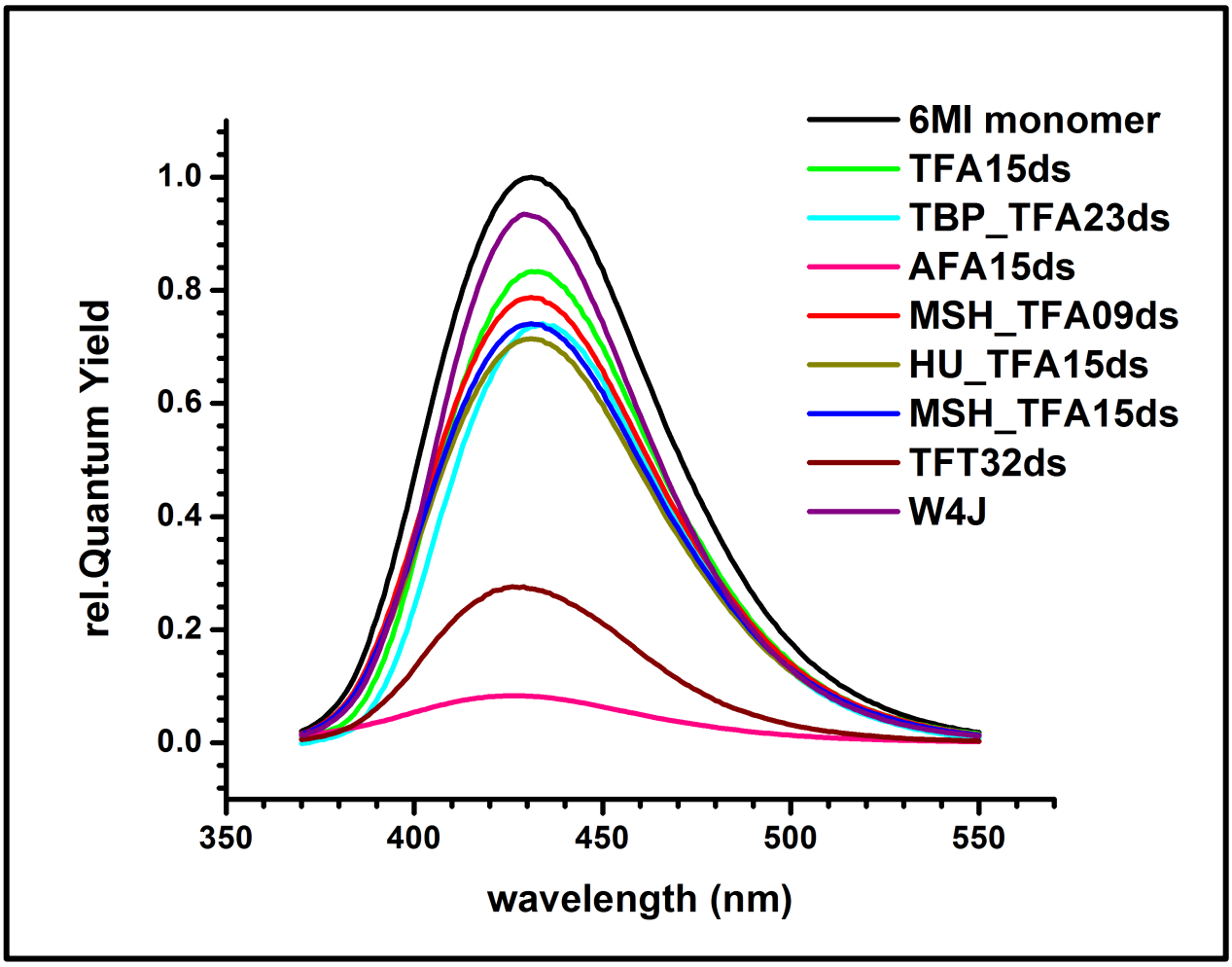

Figure S7. Relative Quantum Yields of 6-MI containing sequences. The quantum yields of different DNA sequences containing 6-MI are shown relative to 6-MI monomer (ex = 340nm) and demonstrate that the enhanced fluorescence observed arises from duplex DNA containing the ATFAA sequence (green, cyan, red, dark yellow, blue, purple). The 6-MI in AFA15ds (magenta) is highly quenched (Q.Y. <0.1). Although formation of the TFT32ds duplex leads to an increase in Q.Y. (0.27), the relative Q.Y. of TFA15ds (green), TBP_TFA23 (cyan), Msh_TFA09 (red), HU_TFA15ds (dark yellow), and Msh_TFA15ds (blue) are at least 0.7 or greater. Also shown is 6-MI fluorescence from a four-way junction construct (4WJ) containing the ATFAA sequence. Enhanced fluorescence is also observed from this construct (Q.Y. ~0.95).

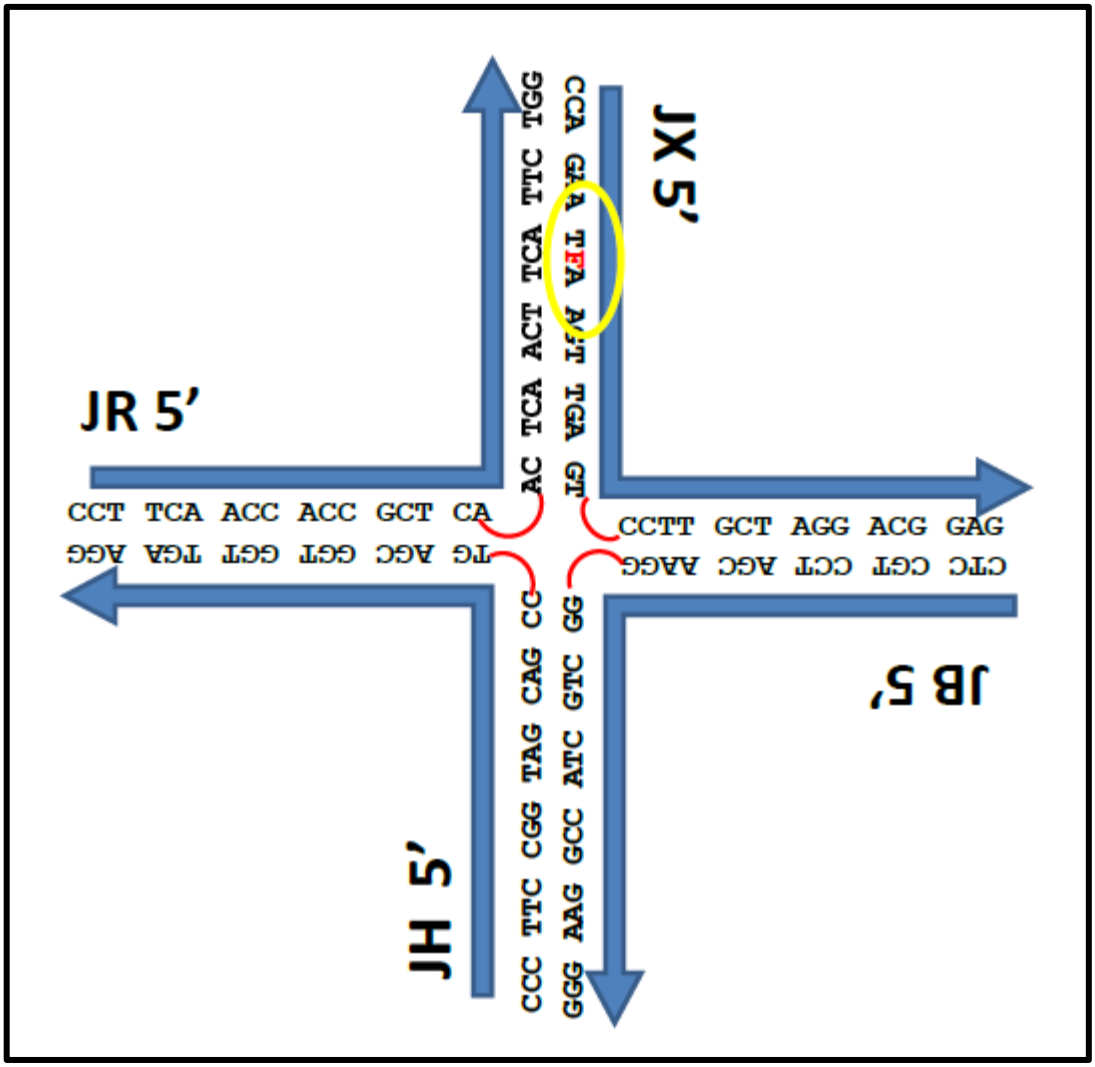

Figure S8. Four-Way Junction containing ATFAA sequence. JX is the oligonucleotide strand containing the pentamer sequence (shown circled in yellow) used to form the 4WJ as shown.

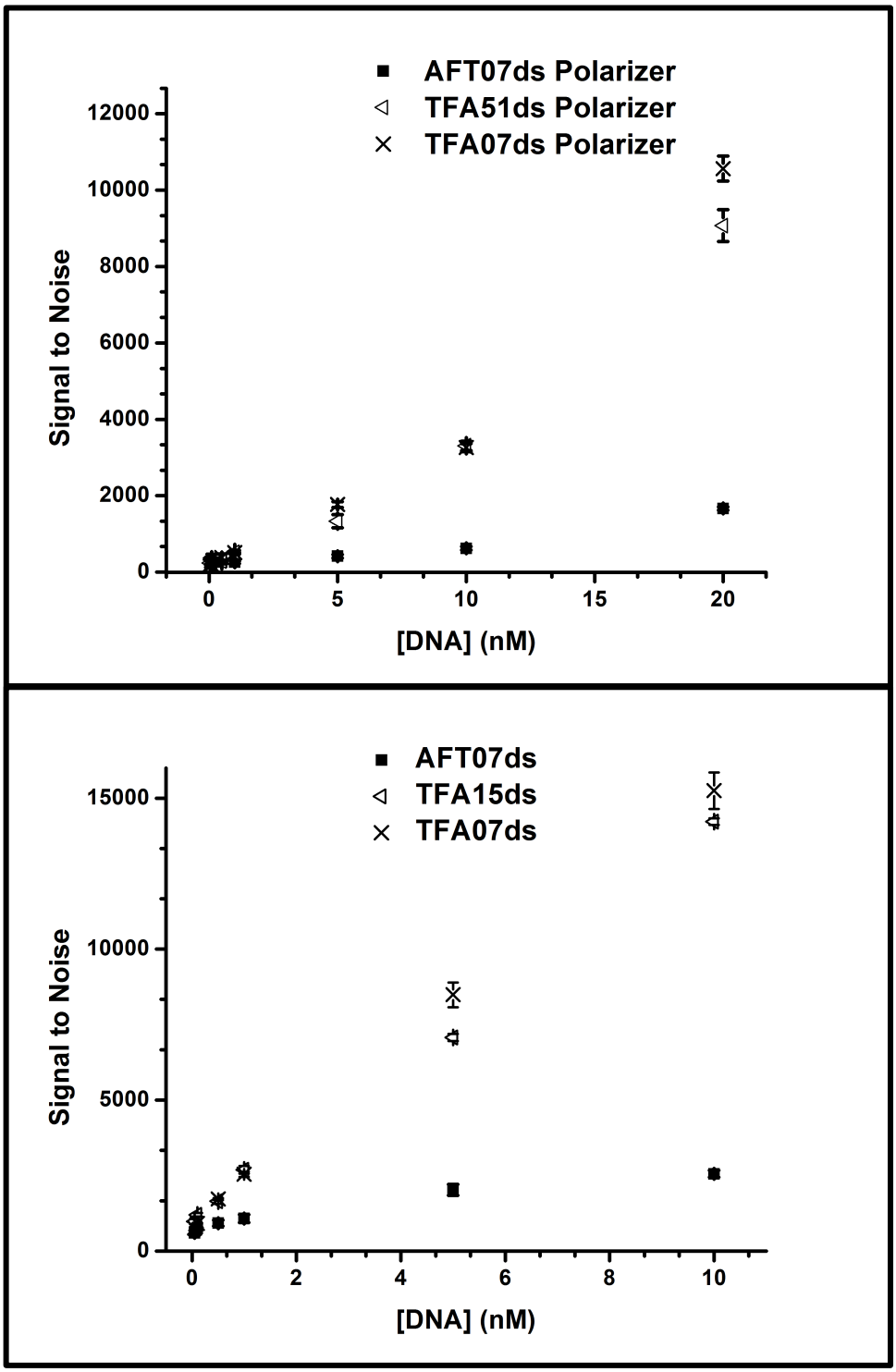

Figure S9. Comparison of sensitivity of different 6-MI duplexes. The signal to noise ratio (S/ √N) measured using protein binding experimental conditions is used to determine the minimum concentration of DNA necessary for accurate measurements. The minimum concentration was defined as the point at which the signal ceases to be linear with concentration. For duplexes exhibiting enhanced 6-MI fluorescence (TFA07, TFA15), the average S/ √N with polarizers at 1nM = 500 and without polarizers at 0.05nM = 900. For the quenched duplex, AFT07ds, the S/ √N is markedly lower, with polarizers at 1nM = 256 and without polarizers at 0.05nM = 598. The S/ √N was calculated as $(I_{signal} - I_{background})/(I_{Background})^{0.5}$. With polarizers present intensity was measured under magic angle conditions (ex = 0°, em = 54.7°)

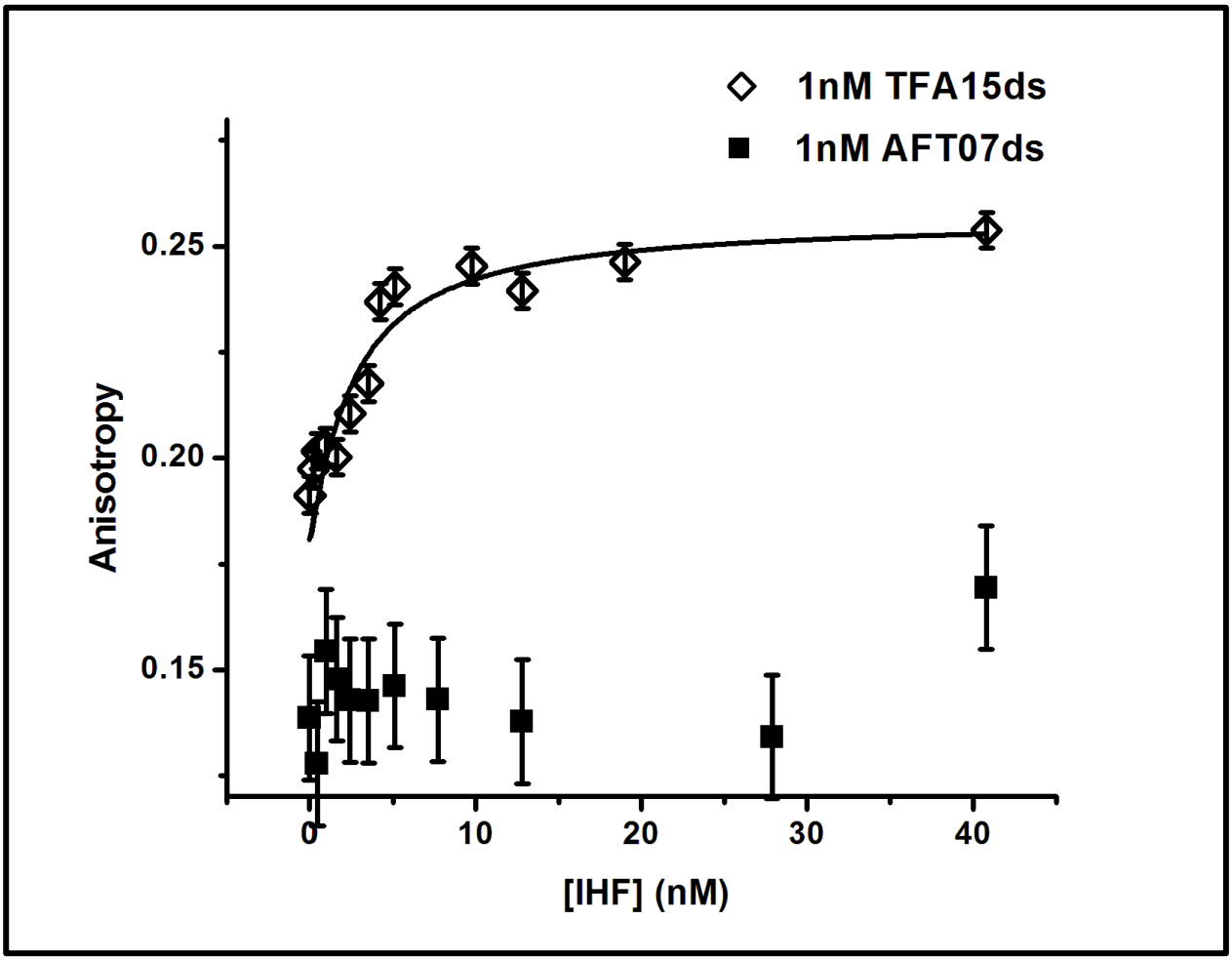

Figure S10. IHF binding measured with 1 nM DNA. The anisotropy binding curves for IHF binding to 1 nM AFT07ds (■) or 1nM TFA15ds (◊) under the same conditions. The low signal of the AFT07ds leads to inaccurate anisotropy measurements as shown by the relatively flat response to increasing protein concentration. The TFA15ds, which exhibits enhanced fluorescence, shows an increase in anisotropy with increasing concentration of IHF consistent with a K_d of 3.7 nM (Table 4). These binding curves demonstrate the benefit of the ATFAA sequence for performing binding measurements with an internal probe at low DNA concentrations.

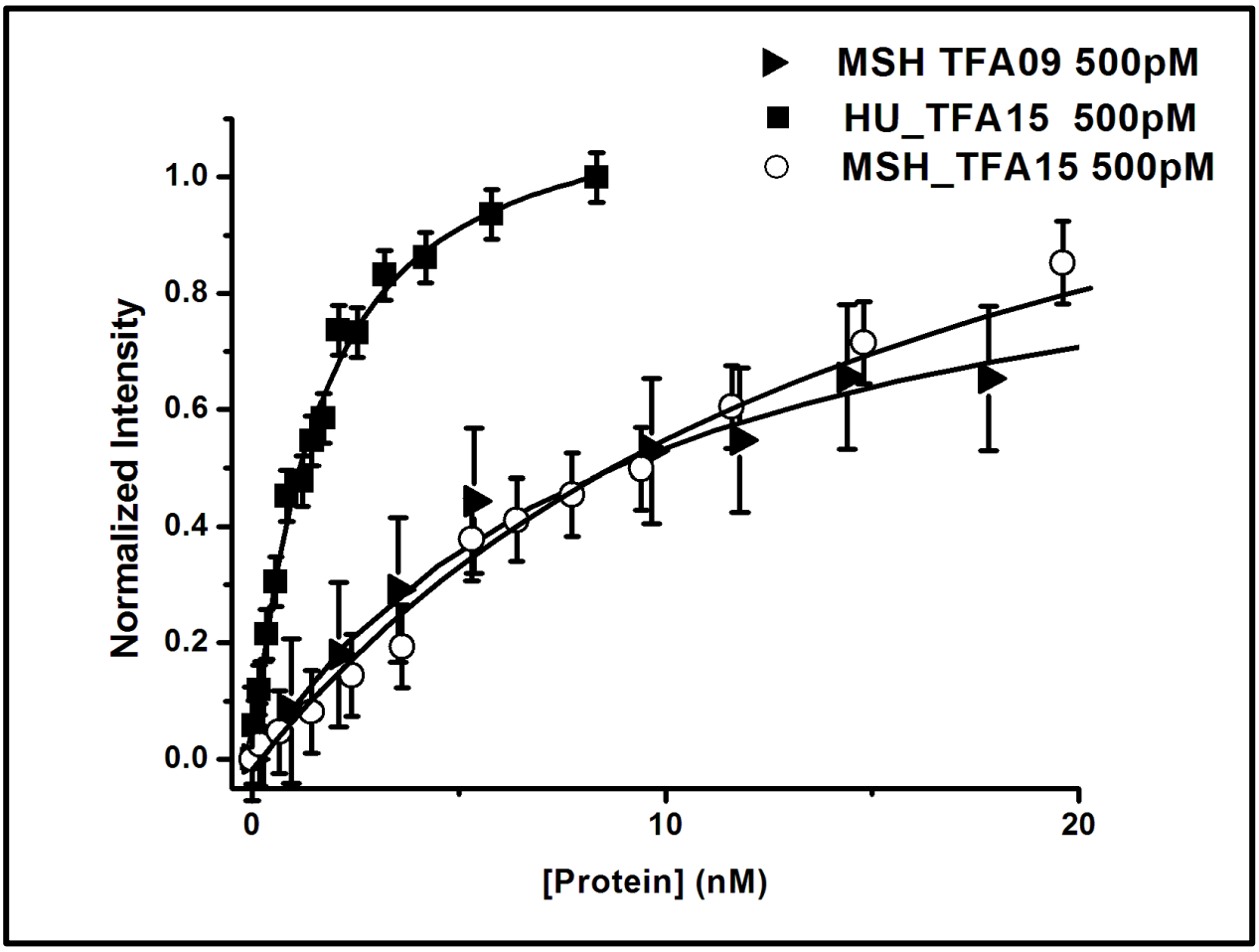

Figure S11. Measurement of Protein binding with 500 pM DNA. Binding curves reveal that the enhanced fluorescence from pentamer ATFAA allows binding measurements to be performed at relatively low DNA concentrations (500 pM and below). At these DNA concentrations the signal is sufficient to accurately measure binding and the dissociation constants obtained are consistent with previously reported values (Table 4).

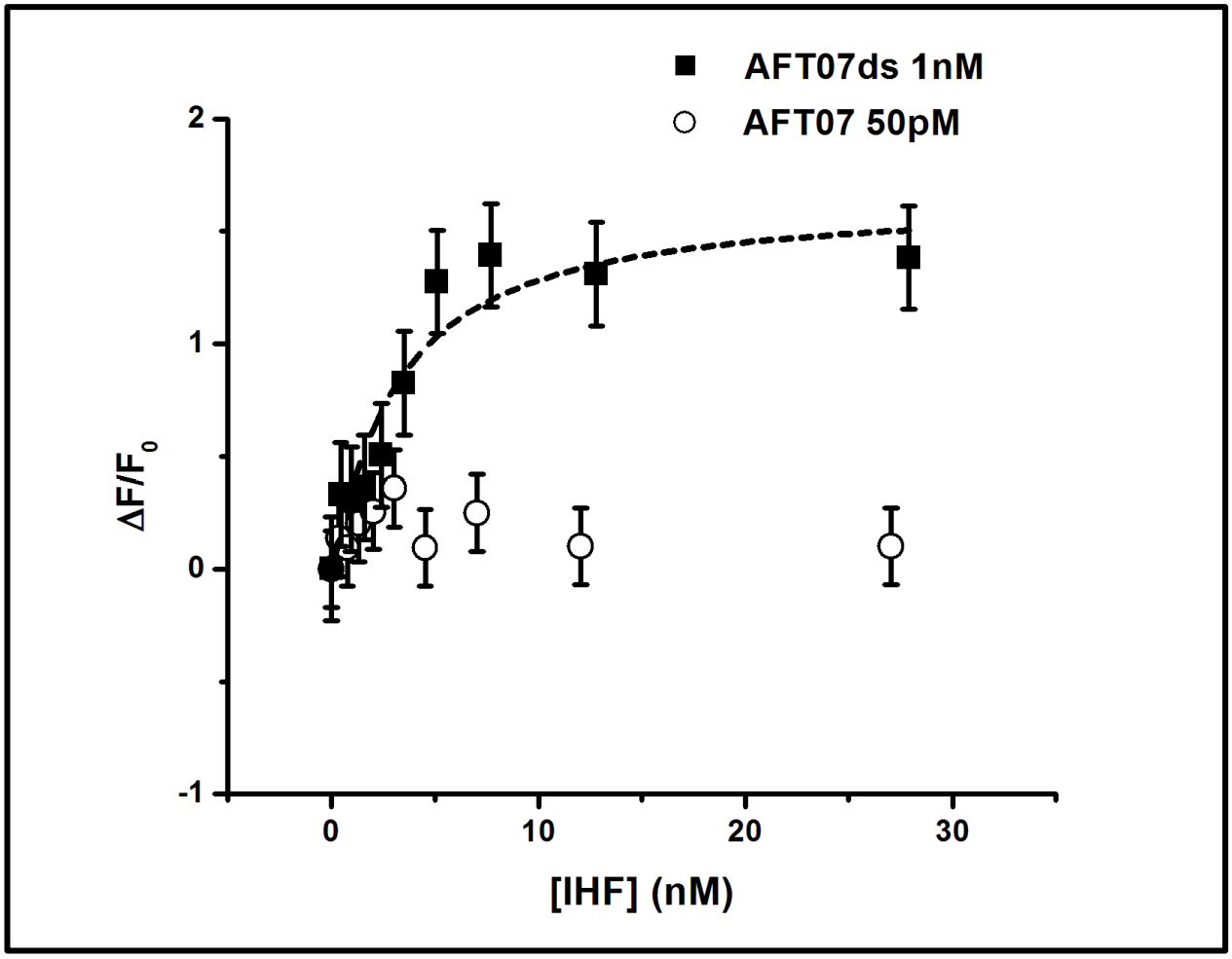

Figure S12. Fluorescence intensity binding curves using 50pM AFT07ds (o) and 1nM AFT07ds (■). The signal of the AFT07ds at 50 pM DNA is not sufficient to measure protein binding accurately as shown by the relatively flat response to protein binding. A 1 nM concentration of DNA is needed to obtain a dissociation constant consistent with previously determined values (K_d = 1.9 ± 0.6 nM) and an intensity change of 130% is observed.

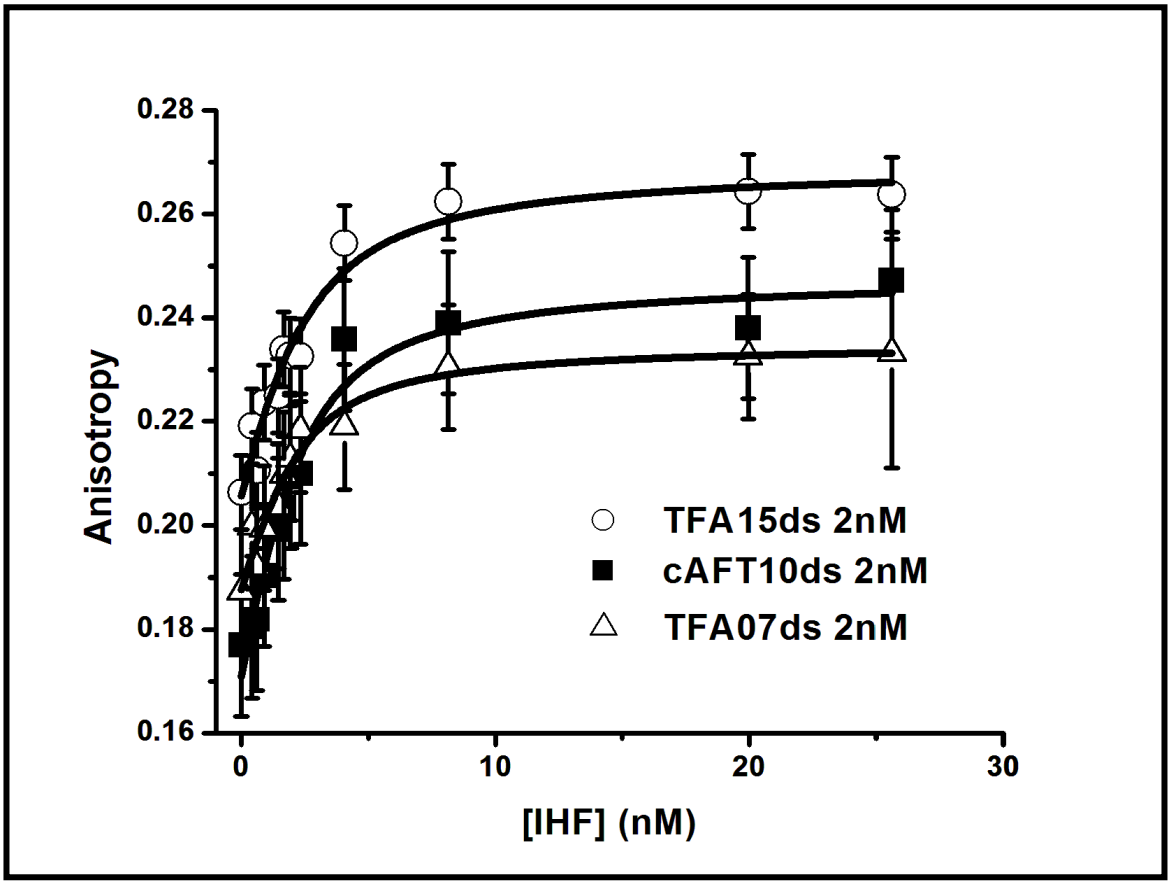

Figure S13. Effect of Probe Position on Anisotropy Measurement. The anisotropy binding curves for IHF binding to DNA with 6-MI labeled in different positions demonstrates binding can be observed independent of probe position in DNA. The relative change in anisotropy is similar for all three constructs. The maximal anisotropy is observed when 6-MI is located in the center of the DNA (TFA15ds).

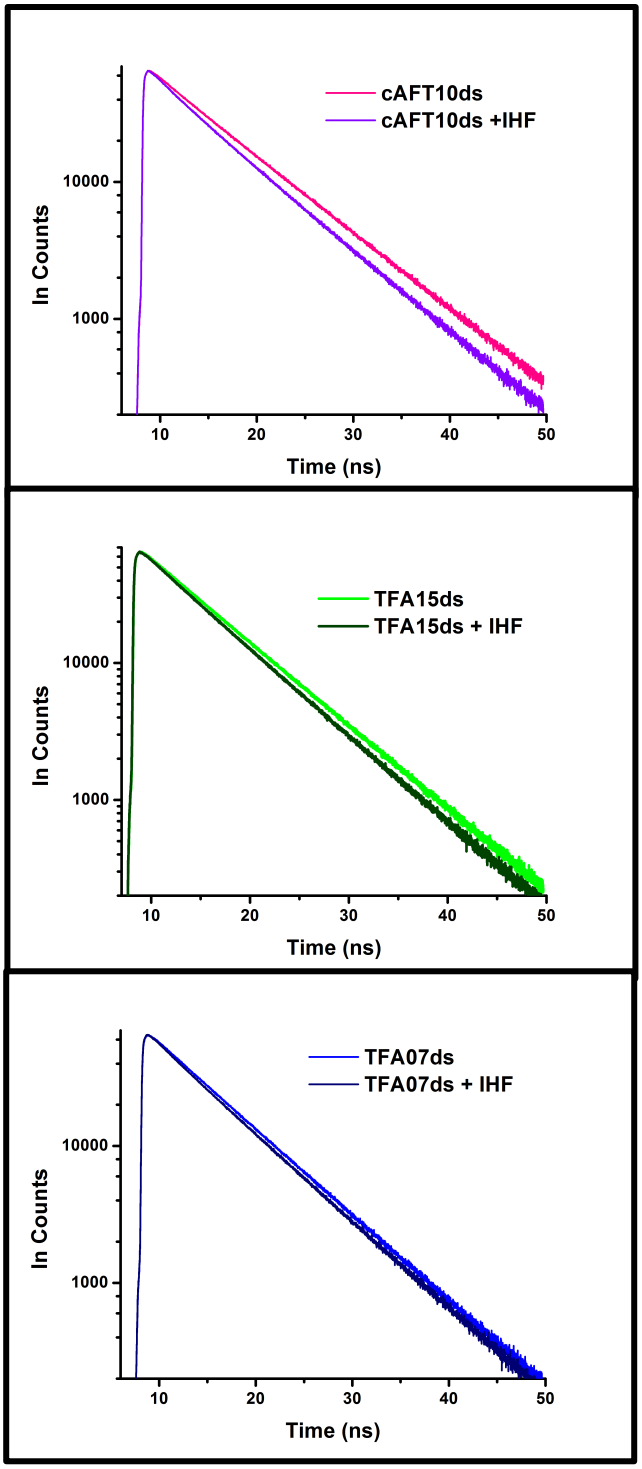

Figure S14. Dynamic Effects of IHF Binding measured by 6-MI. Time-resolved fluorescence spectroscopy (ex=375nm, em=460nm) reveals IHF binding leads to dynamic quenching of 6-MI excited state (purple, dark green, dark blue). The dynamic quenching is greatest when 6-MI is located on the complementary strand in the consensus sequence (cAFT10). There is less quenching as 6-MI is moved further from the consensus sequence, TFA15ds (green, dark green) is adjacent to the consensus and TFA07ds is 8bp away from the consensus sequence (violet, purple).

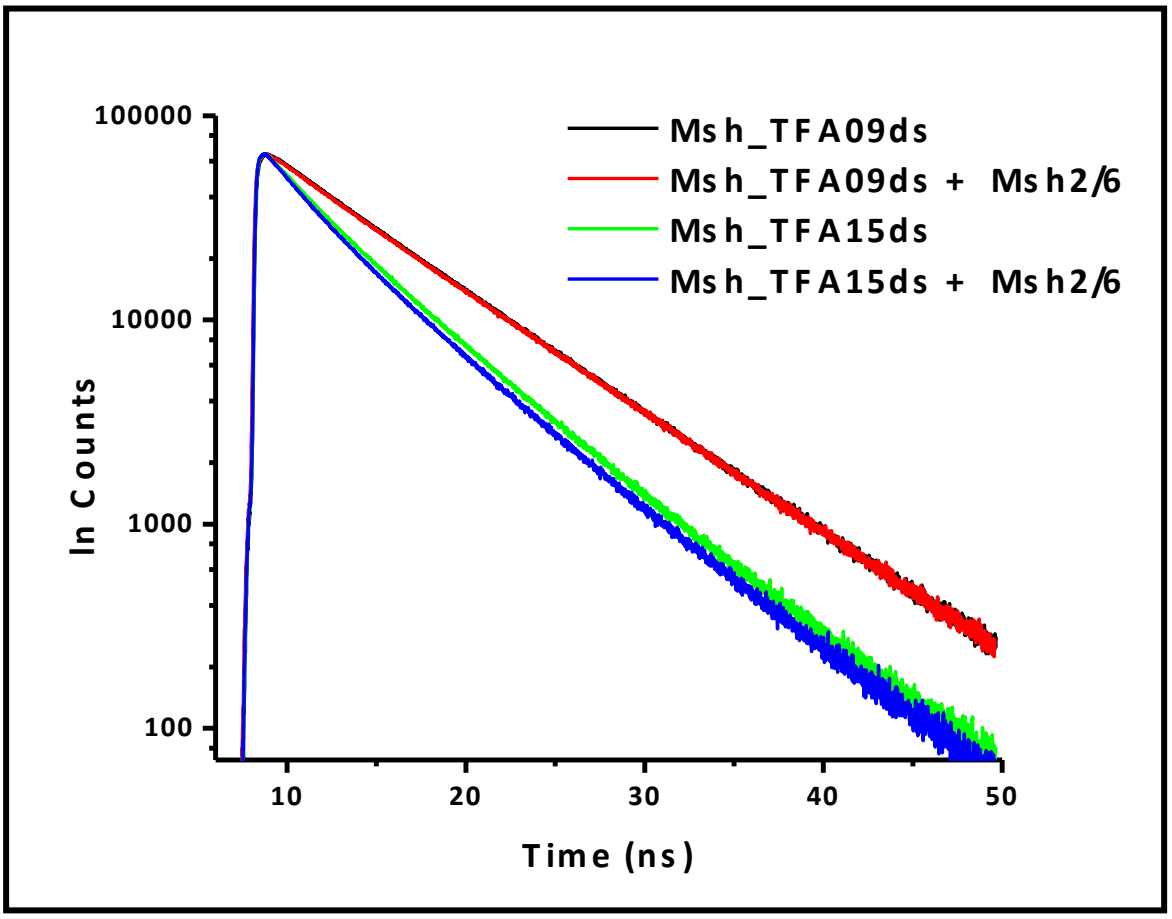

Figure S15. Dynamic Effects of Msh2-Msh6 Binding Measured with 6-MI. Time-resolved fluorescence decay curves (ex=375nm, em=460nm) reveal dynamic quenching of Msh_TFA15ds (blue) with protein binding. This effect is most pronounced when 6-MI was located adjacent to the T-bulge on the 5' side. No detectable dynamic quenching was observed when located 10 basepairs away on the 5' side of T-bulge, Msh_TFA09ds (red with protein, black without protein).

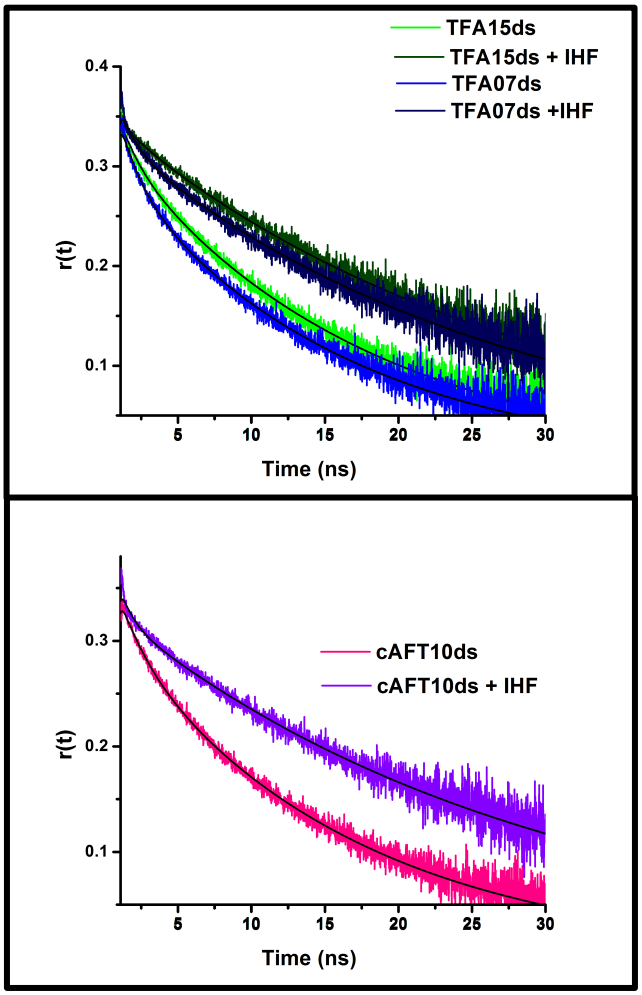

Figure S16. Time-resolved anisotropy decay curves of DNA labeled with 6-MI at three different positions in the presence and absence of IHF indicate local base motion is sensitive to protein binding. For all three duplexes, the overall tumbling time of the DNA (θ_R) is increased with IHF binding as expected (navy blue, dark green, violet). When 6-MI is located in the consensus sequence (bottom), IHF binding leads to an increase in 6-MI local motion (θ_L) (violet).

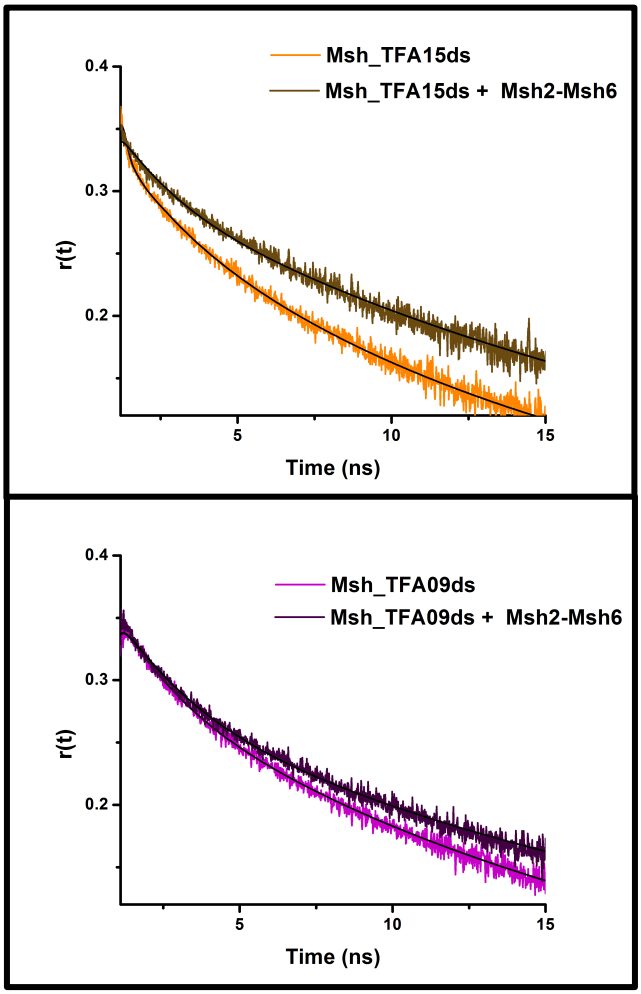

Figure S17. Time-resolved anisotropy decay curves of DNA labeled with 6-MI at two different positions in the presence and absence of Msh2-Msh6 demonstrate 6-MI local motion is sensitive to protein binding. For both duplexes, the overall tumbling time of the DNA (θ_R) is increased with protein binding as expected. Binding to the Msh_TFA15 duplex (orange) leads to a longer correlation time θ_L, suggesting protein binding stabilizes the region around the +T insertion loop (olive green). The absence of a similar increase in θ_L in the Msh_TFA09 duplex, suggests this stabilization is not propagated, but remains close to the +T site (violet, purple).